

# Testing the two planes of satellites in the Centaurus Group

Oliver Müller<sup>1</sup>, Helmut Jerjen<sup>2</sup>, Marcel S. Pawlowski<sup>3</sup>, and Bruno Binggeli<sup>1</sup>

<sup>1</sup> Departement Physik, Universität Basel, Klingelbergstr. 82, CH-4056 Basel, Switzerland  
e-mail: [oliver89.mueller@unibas.ch](mailto:oliver89.mueller@unibas.ch); [bruno.binggeli@unibas.ch](mailto:bruno.binggeli@unibas.ch)

<sup>2</sup> Research School of Astronomy and Astrophysics, Australian National University, Canberra, ACT 2611, Australia  
e-mail: [helmut.jerjen@anu.edu.au](mailto:helmut.jerjen@anu.edu.au)

<sup>3</sup> Department of Astronomy, Case Western Reserve University, 10900 Euclid Avenue, Cleveland, OH 44106, USA  
e-mail: [marcel.pawlowski@case.edu](mailto:marcel.pawlowski@case.edu)

Received tba; accepted tba

## ABSTRACT

**Context.** The existence of satellite galaxy planes poses a major challenge for the standard picture of structure formation with non-baryonic dark matter. Recently Tully et al. (2015) reported the discovery of two almost parallel planes in the nearby Cen A group using mostly high-mass galaxies ( $M_B < -10$  mag) in their analysis.

**Aims.** Our team detected a large number of new group member candidates in the Cen A group (Müller et al. 2016). This dwarf galaxy sample combined with other recent results from the literature enables us to test the galaxy distribution in the direction of the Cen A group and to determine the statistical significance of the geometric alignment.

**Methods.** Taking advantage of the fact that the two galaxy planes lie almost edge-on along the line of sight, the newly found 13 group members by Crnojevic et al. (2014, 2016) and our 16 new Cen A group candidates (Müller et al. 2016) can be assigned relative to the two planes. We use various statistical methods to test whether the distribution of galaxies follows a single normal distribution or shows evidence of bimodality as it has been reported earlier.

**Results.** We confirm that the data used for the Tully et al. (2015) study support the picture of a bimodal structure. However, when the new galaxy samples are included, the gap between the two galaxy planes is closing and the significance level of the bimodality is reduced. Instead, the plane that contains Cen A becomes more prominent.

**Conclusions.** We found evidence that the galaxy system around Cen A is made up of only one plane of satellites. This plane is almost orthogonal to the dust plane of Cen A. Accurate distances to the new dwarf galaxies will be required to measure the precise 3D distribution of the galaxies around Cen A.

**Key words.** galaxies: dwarf, galaxies: groups: individual: Cen A (NGC 5128), Galaxies: individual: Cen A (NGC 5128), large-scale structure of universe

## 1. Introduction

The mere abundance and spatial distribution of faint dwarf galaxies provide a powerful testbed for dark matter and structure formation models on Mpc and galaxy scales. The standard picture of structure formation with dark matter is heavily challenged by the highly asymmetric features found in the distributions of dwarf galaxies in the Local Group. There is the Vast Polar Structure (VPOS, Pawlowski et al. 2012, 2015b; Pawlowski 2016), a thin (rms height  $\approx 30$  kpc) highly inclined, co-rotating sub-structure of faint satellite galaxies, young globular clusters, and stellar streams, spreading in Galactocentric distance between 10 and 250 kpc. A similar feature was found in the Andromeda galaxy surroundings, the so called Great Plane of Andromeda (GPoA, Koch & Grebel 2006; Metz et al. 2007; Ibata et al. 2013). On a slightly larger scale, two dwarf galaxy planes containing all but one of the 15 non-satellite galaxies have been identified in the Local Group (Pawlowski et al. 2013). Such extreme satellite planes are found in only  $< 0.1\%$  of simulated systems in cosmological simulations (e.g. Ibata et al. 2014b; Pawlowski et al. 2014), making them difficult to accommodate in a standard  $\Lambda$ CDM scenario. An alternative analysis of cosmological simulations, based on including the look-elsewhere

effect but ignoring observational uncertainties and the non-satellite planes (Cautun et al. 2015), finds that only about 1 per cent of Local Group-equivalent environments should host similarly extreme satellite structures.

The fundamental question arises whether the relative sparseness and asymmetric distribution of low-mass dwarf galaxies encountered in the Local Group is a statistical outlier, or a common phenomenon in the local universe. Ibata et al. (2014a) have approached this question with a statistical study of velocity anti-correlations among pairs of satellite galaxies on opposite sides of their host, using data from the SDSS survey. They found a strong excess in anti-correlated velocities, which is consistent with co-orbiting planes, but their conclusions were based on a small sample of only 22 systems, and have been challenged since (Phillips et al. 2015). A different approach to address the question of satellite planes is to extend searches for such structures to satellite populations in other galaxy groups in the nearby universe. For example, Chiboucas et al. (2013) have found that dwarf spheroidal galaxies in the M81 group lie in a flattened distribution.

Most recently, Tully et al. (2015), hereafter T15, reported evidence for a double-planar structure around Centaurus A (Cen A, NGC 5128) in the nearby Centaurus Group of galaxies, with properties reminiscent of the two

Local Group dwarf galaxy planes (Pawlowski et al. 2013). Furthermore, Libeskind et al. (2015) found that the Local Group and the Cen A group reside in a filament stretched by the Virgo Cluster and compressed by the Local Void and smaller voids. Four out of five planes of satellites (including the two galaxy planes around Cen A) align with this filament, with the normal vectors pointing in direction of the Local Void and the planes almost parallel to the minor axis of the filament. These results demonstrate that systematic studies of the spatial distribution of low luminosity galaxies in nearby groups can provide important observational constraints for further testing structure formation models outside of the Local Group.

The aim of the present study is to test how recently discovered dwarf galaxies in the Centaurus Group (Sand et al. 2014; Crnojević et al. 2014, 2016; Müller et al. 2015, 2016) are distributed in the double planar structure reported by Tully and collaborators. Comparing the footprint of the two planes, 20 of these dwarf candidates are located in that region of the sky. It is important to note that this analysis is feasible without distance information because of the special geometry: the normal vectors of the two planes are almost parallel and perpendicular to the line-of-sight. Consequently, any distance uncertainties for the new galaxies will not move them in or out of the two planes.

In section 2 we present the four different galaxy samples used in our analysis. In section 3 we show the transformation between the equatorial coordinate system to the Cen A reference frame and fit the two planes of satellites. In section 4 follows a discussion of the geometrical alignment of the planes and the distribution of galaxies. We test the statistical significance of the two planes in Section 5, followed by Section 6 where we summarise the results.

## 2. Sample description

In recent years several untargeted imaging surveys were dedicated to search for low surface-brightness dwarf galaxies in the nearby universe (e.g. Chiboucas et al. 2009, 2013; Merritt et al. 2014; Javanmardi et al. 2016). Especially the richest galaxy aggregate in the Local Volume, the Centaurus A (Cen A) group of galaxies received attention. The PISCeS survey (Sand et al. 2014; Crnojević et al. 2014, 2016) revealed 13 extremely faint dwarf galaxies in the vicinity ( $\sim 11 \text{ deg}^2$ ) of Cen A. Group memberships of nine dwarfs have been confirmed with the tip of the red giant branch (TRGB) method. Our team conducted a survey of 550 square degrees around the Centaurus Group, including the Cen A and M 83 subgroups, discovering 57 potential group member dwarf galaxies (Müller et al. 2015, 2016).

The Centaurus Group is the largest concentration of galaxies in the Local Volume (Distance  $\approx 10 \text{ Mpc}$ ). Before our study there were about 60 group members known (Karachentsev et al. 2004, 2013). Similar to the Local Group, the Centaurus Group has two gravitational centers consisting of a larger galaxy population around the massive, peculiar galaxy NGC 5128 (Cen A) at a mean distance of  $3.8 \text{ Mpc}$ , and a smaller concentration around the giant spiral M 83 at a mean distance of  $4.9 \text{ Mpc}$  (Karachentsev et al. 2004, 2013; Tully et al. 2015; Tully 2015).

This work makes use of four different galaxy samples, they are listed in Table 1. The first sample (1), hereafter called *T15 sample*, is almost identical to the sample of T15 as given in their Table 1. The authors subdivided their

**Table 1.** Galaxy numbers in the four samples. Members and candidates are galaxies with and without distance measurements, respectively.

Sample name	Members (N)	Candidates (N)	Total (N)
T15 sample (1)	14+11	5	30
LV sample (2)	34	0	34
Candidate sample (3)	0	25	25
Complete sample (4)	34	25	59

galaxies into six subsamples: “Plane 1”, “Plane 2”, “Plane 1?”, “Plane 2?”, “other”, and “other?”. The “Plane 1” subsample consists of 14 galaxies. Following T15, we exclude the extremely faint dwarf galaxies Dw-MM-Dw1 and Dw-MM-Dw2 (Crnojević et al. 2014) to avoid any selection bias. The “Plane 2” subsample contains 11 galaxies. In the other four subsamples six galaxies lack measured distance information, meaning that they are considered Cen A members based on morphological and/or surface brightness grounds. From them we exclude PGC 45628 because its projected distance from Cen A is larger than  $1 \text{ Mpc}$ . Three other galaxies (ESO 219-010, ESO 321-014, and PGC 51659) have measured distances but cannot be unambiguously assigned to one of the two planes; we exclude them from the sample. In summary, our *T15 sample* contains 25 galaxies that have measured distances (“members”) and five without (“candidates”).

The second sample (2) includes the 25 members from the *T15 sample* and the nine newly discovered dwarf galaxy members from Crnojević et al. (2014, 2016), including the two PISCeS dwarfs that were excluded in the first sample. Hereafter we call it the *LV sample* because all of these 34 galaxies with distances are part of the Local Volume (LV) sample listed in the online version of the “Updated Nearby Galaxy Catalog” (Karachentsev et al. 2013).

The third sample (3) comprises all candidate members of the Cen A subgroup known to date between  $197.5^\circ < \alpha_{2000} < 207.5^\circ$  and  $-46^\circ < \delta_{2000} < -36^\circ$ . This sample, called hereafter the *Candidate sample*, consists of 25 dwarf candidates in the vicinity of Cen A, including the new dwarf candidates from Müller et al. (2016) and the four candidates without distances from Crnojević et al. (2016). All of these candidates are considered likely members of the Cen A subgroup based on morphological and/or surface brightness grounds.

The fourth sample (4) contains all Cen A group members and candidates known to date, hereafter called the *Complete sample*. It is the combination of the 34 galaxies with distances (*LV sample*) and the 25 candidates from the *Candidate sample*. We note that the *LV sample* and the *Complete sample* contain only galaxies with radial distances smaller than  $1 \text{ Mpc}$  from Cen A ( $3.68 \text{ Mpc}$ ). See Table 2 for a complete list of galaxies (names, coordinates, distances) included in our analysis.

## 3. Transformation between coordinate systems

To compare our results with those of T15 we need to transform the 3D positions of all sample galaxies from the equatorial system to the Cen A reference frame. This is done in three steps: (i) a transformation from equatorial (RA, DEC) to the Galactic ( $l, b$ ) coordinates, (ii) a transforma-

**Table 2.** Members and possible members of the Cen A subgroup.

Galaxy Name	$\alpha_{2000}$ (deg)	$\delta_{2000}$ (deg)	$D$ (Mpc)	Sample	Galaxy Name	$\alpha_{2000}$ (deg)	$\delta_{2000}$ (deg)	$D$ (Mpc)	Sample
ESO269-037 <sup>1</sup>	195.8875	-46.5842	3.15	(1)(2)(4)	CenA-MM-Dw5	199.9667	-41.9936	3.42	(2)(4)
NGC4945 <sup>1</sup>	196.3583	-49.4711	3.72	(1)(2)(4)	CenA-MM-Dw4	200.7583	-41.7861	3.91	(2)(4)
ESO269-058 <sup>1</sup>	197.6333	-46.9908	3.75	(1)(2)(4)	CenA-MM-Dw6	201.4875	-41.0942	3.61	(2)(4)
KKs53 <sup>1</sup>	197.8083	-38.9061	2.93	(1)(2)(4)	CenA-MM-Dw7	201.6167	-43.5567	3.38	(2)(4)
KK189 <sup>1</sup>	198.1875	-41.8319	4.23	(1)(2)(4)	CenA-MM-Dw2	202.4875	-41.8731	3.60	(2)(4)
ESO269-066 <sup>1</sup>	198.2875	-44.8900	3.75	(1)(2)(4)	CenA-MM-Dw1	202.5583	-41.8933	3.63	(2)(4)
NGC5011C <sup>1</sup>	198.2958	-43.2656	3.73	(1)(2)(4)	CenA-MM-Dw3	202.5875	-42.1925	4.61	(2)(4)
KK196 <sup>1</sup>	200.4458	-45.0633	3.96	(1)(2)(4)	CenA-MM-Dw9	203.2542	-42.5300	3.81	(2)(4)
NGC5102 <sup>1</sup>	200.4875	-36.6297	3.74	(1)(2)(4)	CenA-MM-Dw8	203.3917	-41.6078	3.47	(2)(4)
KK197 <sup>1</sup>	200.5042	-42.5356	3.84	(1)(2)(4)	dw1315-45	198.9833	-45.7506	3.68*	(3)(4)
KKs 55 <sup>1</sup>	200.5500	-42.7308	3.85	(1)(2)(4)	dw1318-44	199.7417	-44.8947	3.68*	(3)(4)
NGC5128 <sup>1</sup>	201.3667	-43.0167	3.68	(1)(2)(4)	CenA-MM-Dw11	200.4167	-43.0825	3.68*	(3)(4)
KK203 <sup>1</sup>	201.8667	-45.3525	3.78	(1)(2)(4)	dw1322-39	200.6333	-39.9060	3.68*	(3)(4)
ESO324-024 <sup>1</sup>	201.9042	-41.4806	3.78	(1)(2)(4)	dw1323-40c	200.9042	-40.7214	3.68*	(3)(4)
NGC5206 <sup>2</sup>	203.4292	-48.1511	3.21	(1)(2)(4)	dw1323-40b	200.9792	-40.8358	3.68*	(3)(4)
NGC5237 <sup>2</sup>	204.4083	-42.8475	3.33	(1)(2)(4)	CenA-MM-Dw12	201.0417	-42.1397	3.68*	(3)(4)
NGC5253 <sup>2</sup>	204.9792	-31.6400	3.55	(1)(2)(4)	dw1323-40	201.2208	-40.7614	3.68*	(3)(4)
KKs 57 <sup>2</sup>	205.4083	-42.5819	3.83	(1)(2)(4)	dw1326-37	201.5917	-37.3856	3.68*	(3)(4)
KK211 <sup>2</sup>	205.5208	-45.2050	3.68	(1)(2)(4)	CenA-MM-Dw10	201.7042	-43.0000	3.68*	(3)(4)
KK213 <sup>2</sup>	205.8958	-43.7691	3.77	(1)(2)(4)	dw1329-45	202.2917	-45.1753	3.68*	(3)(4)
ESO325-011 <sup>2</sup>	206.2500	-41.8589	3.40	(1)(2)(4)	CenA-MM-Dw13	202.4625	-43.5194	3.68*	(3)(4)
KK217 <sup>2</sup>	206.5708	-45.6847	3.50	(1)(2)(4)	dw1330-38	202.6708	-38.1675	3.68*	(3)(4)
CenN <sup>2</sup>	207.0375	-47.5650	3.66	(1)(2)(4)	dw1331-40	202.8583	-40.2631	3.68*	(3)(4)
KK221 <sup>2</sup>	207.1917	-46.9974	3.82	(1)(2)(4)	dw1331-37	202.8833	-37.0581	3.68*	(3)(4)
ESO383-087 <sup>2</sup>	207.3250	-36.0614	3.19	(1)(2)(4)	dw1336-44	204.1833	-44.4472	3.68*	(3)(4)
KK198	200.7342	-33.5728	3.68*	(1)(3)(4)	dw1337-44	204.3917	-44.2186	3.68*	(3)(4)
KKs54	200.3850	-31.8864	3.68*	(1)(3)(4)	dw1337-41	204.4792	-41.9031	3.68*	(3)(4)
KKs59	206.9920	-53.3476	3.68*	(1)(3)(4)	dw1341-43	205.4042	-43.8547	3.68*	(3)(4)
KKs58	206.5042	-36.3281	3.68*	(1)(3)(4)	dw1342-43	205.6633	-43.2553	3.68*	(3)(4)
KKs51	191.0896	-42.9397	3.68*	(1)(3)(4)					

**Notes.** Galaxies with unknown distances are marked with a “\*”. We adopted the distance of Cen A (3.68 Mpc) for them. Galaxies which are members of Plane 1 or 2 are marked with “<sup>1</sup>” or “<sup>2</sup>”, respectively, according to T15. Denoted with (1) are galaxies belonging to the *T15 sample*, (2) are galaxies from the *LV sample*, (3) are candidate galaxies belonging to the *Candidate sample* and (4) are galaxies in the *Complete sample*.

tion to the supergalactic (SGL, SGB) coordinates and (iii) a translation and rotation to the Cen A reference frame (CaX, CaY, CaZ). In the latter reference system, Cen A is located at the origin, and the two nearly parallel galaxy planes, represented by an averaged normal direction, lie in the XY projection. The two planes are then visible edge-on in the XZ projection (see our Sect. 4 and Fig. 2 in T15).

The transformation between polar coordinates and Carthesian coordinates is given by:

$$x = d \cdot \cos(\delta) \cdot \cos(\alpha)$$

$$y = d \cdot \cos(\delta) \cdot \sin(\alpha)$$

$$z = d \cdot \sin(\delta)$$

where  $d$  is the heliocentric distance to the galaxy. To rotate from equatorial coordinates to Galactic coordinates, the Carthesian coordinates  $v = (x, y, z)$  (equatorial system) have to be multiplied from the left by the rotation matrix:

$$\mathbf{R}_G = \begin{bmatrix} -0.0549 & -0.8734 & -0.4839 \\ +0.4941 & -0.4448 & +0.7470 \\ -0.8677 & -0.1981 & +0.4560 \end{bmatrix}$$

From galactic coordinates to supergalactic coordinates the rotation is given by the matrix:

$$\mathbf{R}_{SG} = \begin{bmatrix} -0.7357 & +0.6773 & +0.0000 \\ -0.0746 & -0.0810 & +0.9940 \\ +0.6731 & +0.7313 & +0.1101 \end{bmatrix}$$

Therefore the transformation from equatorial to supergalactic coordinates is:

$$v_{SG} = \mathbf{R}_{SG} \mathbf{R}_G v$$

T15 transformed the supergalactic coordinates into the Cen A reference frame. To do this, they applied a translation to the coordinate system such that Cen A is at the origin (0,0,0):

$$v_{SG, CenA} = v_{SG} + \begin{pmatrix} +3.41 \\ -1.26 \\ +0.33 \end{pmatrix} [\text{Mpc}]$$

and then rotate into the new coordinate system with:

$$\mathbf{R}_{Ca} = \begin{bmatrix} +0.994 & -0.043 & +0.102 \\ -0.001 & +0.919 & +0.393 \\ -0.111 & -0.391 & +0.914 \end{bmatrix}$$

The final transformation to the Cen A reference frame is:

$$v_{Ca} = \mathbf{R}_{Ca} v_{SG, CenA}$$

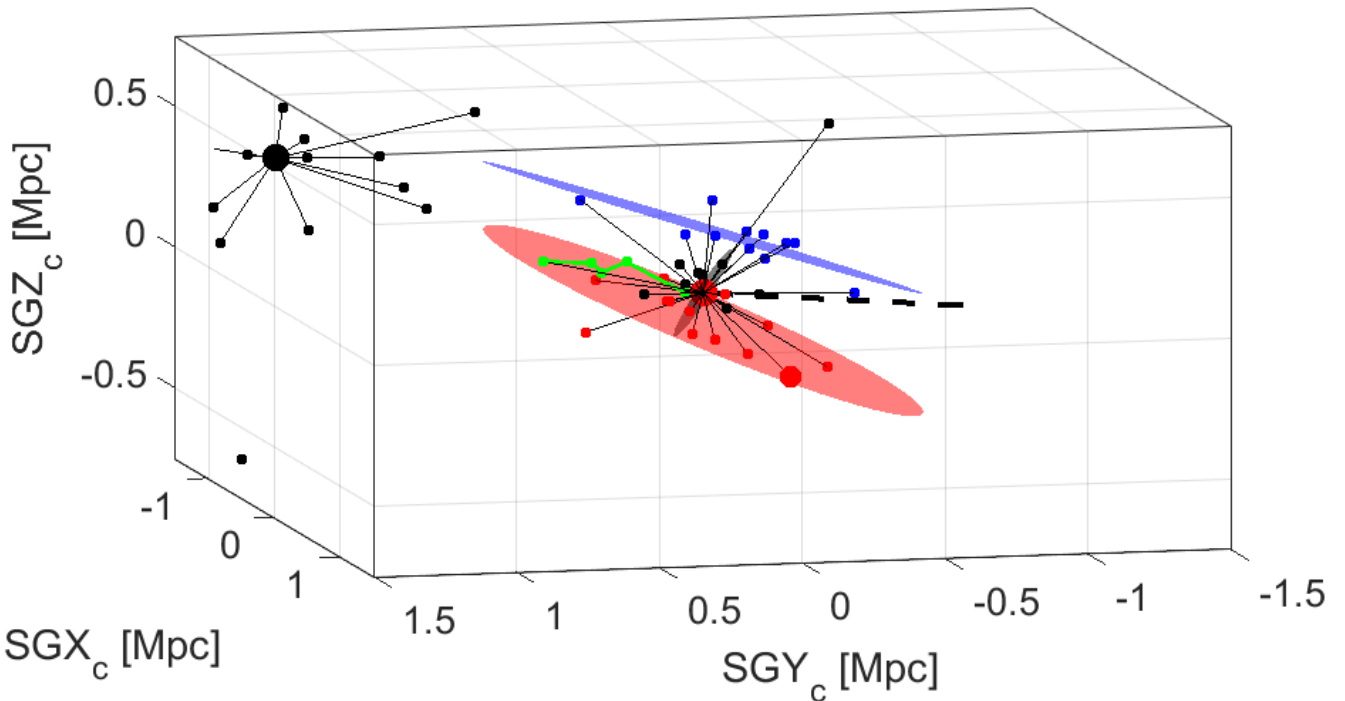


**Fig. 1.** 3D distribution of known Centaurus group members in supergalactic coordinates centered on Cen A. The large red dot is Cen A, the large black dot is M 83, and the intermediate-size red dot is the late-type spiral NGC 4945. The small red dots are plane 1 dwarf satellite members, the blue dots plane 2 members from T15, the black dots are additional (non-plane) members of the Cen A group. The best-fitting planes 1 and 2 are illustrated by the red and blue disks, respectively. The smaller grey disk which stands almost orthogonal to the two satellite planes represents the dust lane of Cen A. The dashed black line corresponds to the line of sight towards Cen A. The green line connects the five regions in the tail of the tidally disrupted dwarf CenA-MM-Dw3 where distances could be measured (Dw3, Dw3 S, Dw3 SE, Dw3 N, and Dw3 NW, Crnojević et al. 2016).

#### 4. Geometrical alignment of the satellites

We used two different algorithms to fit the two planes of satellites in three dimensions: (1) a singular value decomposition (svd, Golub & Kahan 1965) and (2) the tensor of inertia (ToI, e.g. Pawłowski et al. 2015a). The 14 galaxies used for fitting plane 1 are labeled with “1” in Table 2, the 11 galaxies for plane 2 with “2”. The normal vectors of the best-fitting planes given in supergalactic coordinates are  $\mathbf{n}_1 = (-0.1576, -0.4306, 0.8886)$  and  $\mathbf{n}_2 = (0.0875, 0.3225, -0.9425)$  for plane 1 and 2, respectively. Both algorithms return the same results. The angle between the two normal vectors is found to be  $8.0^\circ$ , in good agreement with  $7^\circ$  published by T15. Why there is a difference with T15 at all cannot be evaluated, as neither the plane-fitting method nor the exact sample of galaxies used for the fits have been stated in T15. The measured angles between  $\mathbf{n}_1$ ,  $\mathbf{n}_2$ , and the normal vector of the supergalactic plane are  $16.9^\circ$  and  $24.6^\circ$ , respectively, meaning that the two planes are not far from being parallel to the supergalactic plane. Using the ToI algorithm we further calculated that plane 1 has a root-mean-square (rms) thickness of 69 kpc and a major-axis rms length of 309 kpc, while plane 2 has a thickness of 48 kpc and a length of 306 kpc.

As the prominent dust lane of Cen A itself represents a reference plane, one can further ask how the satellite planes are spatially arranged with respect to Cen A. The orientation of the dust lane was studied by Hui et al. (1995) who

give an inclination of  $17^\circ$  to the line of sight and a position angle for the disk angular momentum of  $35^\circ$  in the sky (counting from N through E). This latter angle also coincides with the position angle of the photometric major axis (Dufour et al. 1979). From these two angles we calculated the normal vector of the Cen A dust plane in supergalactic coordinates to be  $\mathbf{n}_{\text{dust}} = (-0.0305, 0.8330, 0.5525)$ . The resulting angular difference to the normal vectors of the satellite planes 1 and 2 amounts to  $82.1^\circ$  and  $104.8^\circ$ , respectively. This means that the satellite planes are almost orthogonal to the dust plane of Cen A (see Fig. 1) – reminiscent of the local situation where the Vast Polar Structure is essentially perpendicular to the plane of the Milky Way. We further note that the angle between the connection line of Cen A and M 83 and the normal of the dust plane is only  $30^\circ$ , meaning that  $\mathbf{n}_{\text{dust}}$  almost points towards M 83.

Crnojević et al. (2016) discovered the tidally disrupted dwarf galaxy CenA-MM-Dw3 with tails spanning over  $1^\circ.5$  ( $\sim 120$  kpc). They measured distances at five separate high surface brightness locations along the elongation. Defining the directional vector of CenA-MM-Dw3 as the vector between CenA-MM-Dw3 and CenA-MM-Dw3-SE, the vector is  $\mathbf{e}_{\text{Dw3}} = (0.8983, -0.4266, 0.1056)$  in supergalactic coordinates. Astonishingly, we find that angles between this vector and the plane 1 and 2 normal vectors are  $82^\circ$  resp.  $99^\circ$ , meaning that the tidally disrupted dwarf is almost parallel to the two planes. This is again reminiscent of the Local Group where the Magellan Stream aligns with the VPOS.

In contrast to the Local Group the angle between  $\mathbf{e}_{\text{Dw3}}$  and the normal of the dust plane is  $109^\circ$ , meaning that the tidal dwarfs is almost parallel to the dust plane. The tail itself lies along the line of sight, having the positive effect that the distance errors only move along this direction, hence the uncertainties do not change the angles between the tail and the planes. In Table 3 we compile the calculated vectors in supergalactic coordinates.

**Table 3.** Directions in supergalactic coordinates.

(SGX, SGY, SGZ)		
normal plane 1	$\mathbf{n}_1$	(−0.1576, −0.4306, +0.8886)
normal plane 2	$\mathbf{n}_2$	(+0.0875, +0.3225, −0.9425)
normal Cen A dust	$\mathbf{n}_{\text{dust}}$	(−0.0305, +0.8330, +0.5525)
elongation Dw3	$\mathbf{e}_{\text{Dw3}}$	(+0.8983, −0.4266, +0.1056)

Fig. 1 shows the 3D galaxy distribution of the Centaurus Group in supergalactic coordinates, with Cen A at the origin. Data are drawn from the online version of the LV catalog (Karachentsev et al. 2013). Note the primary double structure of the group defined by the Cen A (big red dot) subgroup and the M 83 (big black dot) subgroup, and the secondary double-plane structure around the Cen A subgroup. The 14 “Plane 1” satellites are shown as red dots, the 11 “Plane 2” satellites as blue dots according to the *T15 sample*. The intermediate-size red dot is NGC 4945. Indicated are also the best-fitting planes (shown as red and blue disks; for details on the fitting procedure see above), the alignment of the tidal features of CenA-MM-Dw3 (green line with dots), as well as the dust plane of Cen A (in grey).

## 5. Mapping the new dwarf candidates

We now switch to the Cen A reference frame (CaX, CaY, CaZ) that was introduced by T15. The top panels of Fig. 2 show the distribution of the Cen A group members in the CaX – CaZ projection, a plot that is directly comparable to Fig. 2 of T15. Here, the two galaxy planes are seen edge-on. The bottom panels show the CaX – CaY projection, presenting the planes in a face-on view. As it has been already noted in T15, our line of sight lies almost in the direction of the two planes. The angle between the best-fitting planes and the line of sight at the distance of Cen A is only  $14.6^\circ$  and  $12.8^\circ$  (with a different sign), respectively for plane 1 and 2. As a consequence of this geometry, any distance uncertainties move galaxies essentially along the two planes and thus have little bearing on the bimodal structure. On the other hand, for the same reason one might surmise that the planes are an artifact produced by the spread of distance errors. However, this is unlikely the case, as the planes are significantly more extended than the distance errors. T15 came to the same conclusion.

The special geometrical situation allows us to put the two planes of satellites to the test with the help of our new dwarf candidates around Cen A (Müller et al. 2016). Given the celestial position (i.e. equatorial coordinates) of a dwarf candidate, its relative position to the planes is essentially given too. There are three possibilities for a candidate: (1) it lies in one of the two planes, (2) it lies between the planes, or (3) it lies outside of the bimodal structure. Again, the key

point is that this test can be conducted without knowing the distances of the candidates, deferring, at least in this preliminary manner, the time-consuming task of distance measurements.

In the top panels of Fig. 2 all known Cen A group members with distances are plotted in the CaX – CaZ projection. Red dots are the galaxies in plane 1, blue dots are galaxies in plane 2 according to T15, black triangles are the newly found galaxies by Crnojević et al. (2014, 2016). The best-fitting planes, i.e. their lines of intersection with the orthogonal CaX – CaZ plane, are shown in the top left panel. In the top right panel the 5 percent distance uncertainties for the galaxies are added, showing the distance range along the line of sight. Likewise, the thin black lines in the top left panel indicate the lines of sight for the candidate Cen A group members, nicely illustrating the near parallelism between the satellite planes and our line of sight. The bottom panels show the CaX – CaY projection, looking at the plane face-on.

From the CaX – CaZ projection it becomes clear that the 25 dwarf galaxy candidates, provided they are Cen A group members, can be assigned almost unambiguously to one of the two planes, because there is no double plane crossing along the line of sight at the distance of Cen A. In fact, of the 25 lines of sight (= possible positions of the candidates) none is crossing both planes within the distance range considered ( $D_{\text{Cen A}} \pm 0.75$  Mpc), see Fig. 2, top left. One candidate, KKs 51, is clearly missing both planes. For example, to be a member of plane 1, it would have to be 2 Mpc from the Milky Way (or 1.9 Mpc from Cen A) where the line of sight and plane 1 intersect. In T15 this candidate is marked as *other?*. We conclude that KKs 51 is not a member of the planes and therefore should count as *other*. Looking solely at the CaX-CaZ projection, there remains the possibility that the lines of sight are only projected into the region of the planes, while in the 3D reality they could lie way off the planes. The CaX-CaY projection (face-on view) in the bottom panels shows that this is not the case. Only the line of KKs 51 is far from the Cen A galaxy aggregation.

Interestingly, the nine PiSCeS dwarfs (black triangles in Fig. 2) seem to fill the gap between the two planes. This raises the question what will happen when the large sample of our new dwarf candidates comes into play. Will the bimodal structure be lost altogether, unmasking the promising double-plane structure of the Cen A subgroup as an effect of small-number statistics, or will the case for a double-plane be strengthened?

The Cen A subgroup members and candidates can now be sampled along the CaZ axis. In T15 this is done in their Fig 2 by plotting a histogram of CaZ coordinates for members with their individually measured distances and for possible members (the dwarf candidates) assuming a distance of 3.68 Mpc (the distance of Cen A). We have binned our galaxy samples in the same way in Fig 3. The red and blue bins correspond to the plane galaxies from the *T15 sample*, coloured as before. The bimodal structure is clearly visible. If we add the nine satellites (in black) from the PiSCeS survey (Crnojević et al. 2014, 2016) the gap starts to fill up. A limitation of the PiSCeS survey, however, is the relatively small area of  $11 \text{ deg}^2$  covered (see Fig. 2 in Müller et al. 2016). Nevertheless, inspite of this possible bias, every dwarf which is found between the two planes does reduce the significance of the bimodality. Finally when including

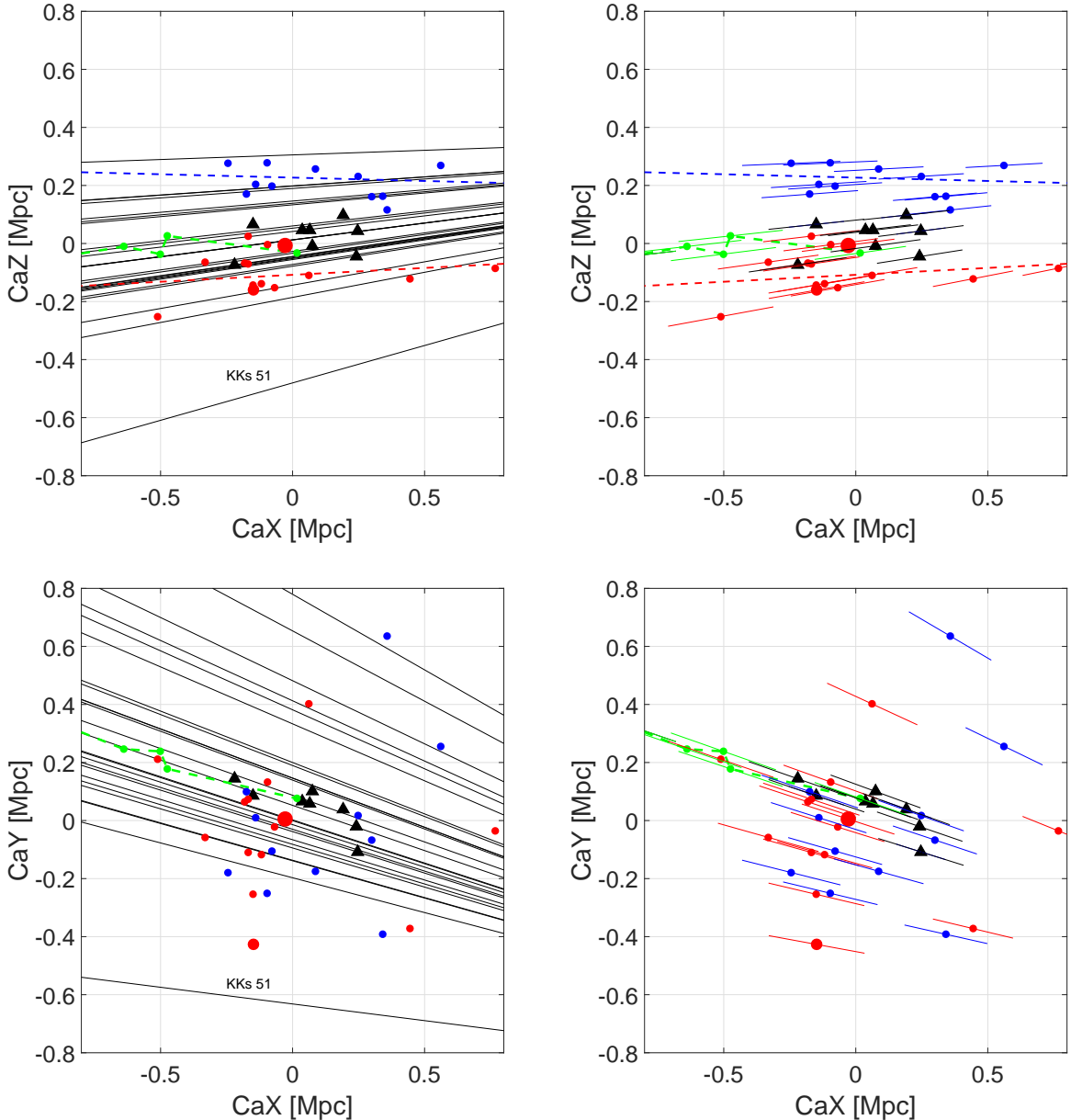


**Fig. 2.** Top left: edge-on view of the two galaxy planes. Red dots are satellites in plane 1, blue dots are satellites in plane 2, black triangles are new dwarfs from the PISCeS survey. The green dotted line corresponds to the tidally disrupted dwarf CenA-MM-Dw3 where the dots themselves are regions in the tail where distances were measured (Dw3 S, Dw3 SE, Dw3 N, and Dw3 NW). CenA-MM-Dw3 itself is falling outside the frame. The red and blue dashed lines are the best-fitting planes. The 25 thin black lines indicate the possible locations of new dwarf candidates without distance measurements. Top right: same as top left but without the possible group members, giving instead an indication of the distance uncertainties of the known members. The colored lines correspond to a 5 percent distance errors, projected onto the CaX - CaZ plane. Bottom left: galaxy distribution in the CaX - CaY plane, where we see the two planes superimposed and face-on. Bottom right: Same as bottom left, only showing the galaxies with known distances. As in Fig. 1, the large red dot is Cen A and the intermediate-size red dot is the giant spiral NGC 4945.

the more homogeneous and bias-free sample of 25 candidates (grey bins) that covers most of the vicinity of Cen A from the *Candidate sample* (Müller et al. 2016; Crnojević et al. 2016) the bimodality in the distribution increases slightly again and the population of plane 1 becomes the dominant.

However, we note that this representation of the CaZ distribution as a histogram is somewhat problematic. Not only does a histogram depend on the chosen starting point

and bin width, we also have adopted the same fixed distance for all candidates. Although there is only a weak dependence of CaZ on the distance, owed to the fact that the line of sight is almost perpendicular to the CaZ axis, the mean CaZ range covered by a group member candidate is around 0.11 Mpc in the distance interval  $2.93 < D < 4.43$  Mpc, which can shift a candidate back and forth by up to two bins of 0.05 Mpc width. A better representation of the data can be achieved by using the adaptive kernel density estimation.

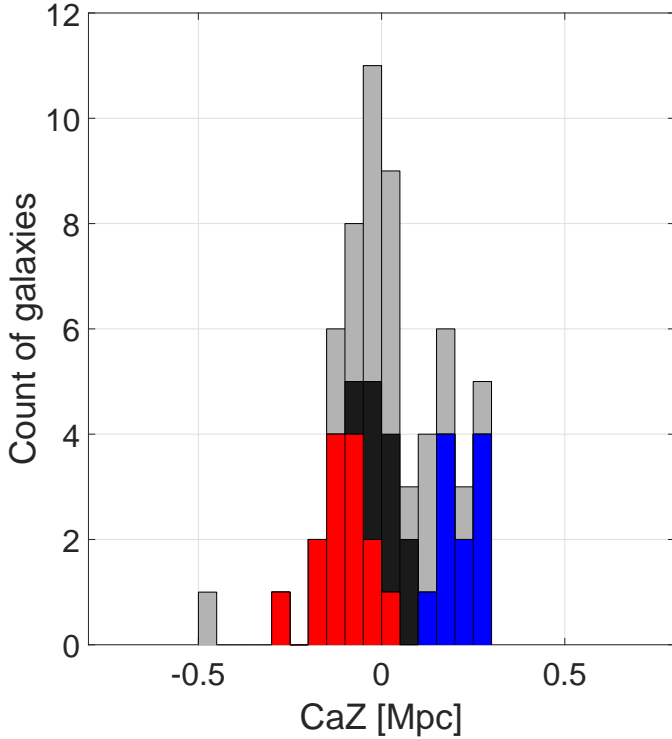


**Fig. 3.** Histogram of the Cen A satellite distribution along the CaZ axis. The red and blue bins correspond to the (14+11) plane 1 and 2 members, respectively, from the T15 sample. The grey bins are the 25 Cen A subgroup member candidates assuming a distance of 3.68 Mpc (Cen A).

In this technique, the galaxies (members and candidates) are represented by standard normal curves with  $\mu$  as the measured or assumed distance and  $\sigma$  as the distance uncertainty amounting to 5 percent for members, accounting for measurement errors, and 0.5 Mpc for candidates, accounting for the depth of the subgroup. The standard normal curves are then projected onto the CaZ axis, resulting in standard normal curves with different  $\sigma$  values, which depend on the projection angle, i.e. the angle between the line of sight and CaZ. This angle varies systematically over CaZ (see Fig. 2, top left), from close to orthogonal at positive CaZ values (CaZ  $\sim$  0.2 Mpc), giving very narrow standard curves, to ever smaller acute angles towards negative CaZ values (CaZ  $\sim$  -0.3 Mpc), giving broader standard curves. The combined density distribution of the galaxies along the CaZ axis, by co-adding the projected normal curves is given in Figs. 4 and 5.

In Fig. 4 the *T15 sample* (black solid line) and all candidate galaxies without distances from the *Candidate sample* (red dashed line) are plotted differentially. For the galaxies without distance measurements a distance of 3.68 Mpc and a distance uncertainty of  $\pm 0.5$  Mpc is assumed. These standard normal curves are plotted in grey. The bimodality is visible, albeit the peak around plane 1 is higher than the peak around plane 2.

Fig. 5 shows the same data as the histogram in Fig. 3. This plot contains all the information up to date. The grey line corresponds to the plane satellites from the *T15 sample*, the black line to the *LV sample* and the red dashed line to the *Complete sample*. In all three samples the gap is visible.

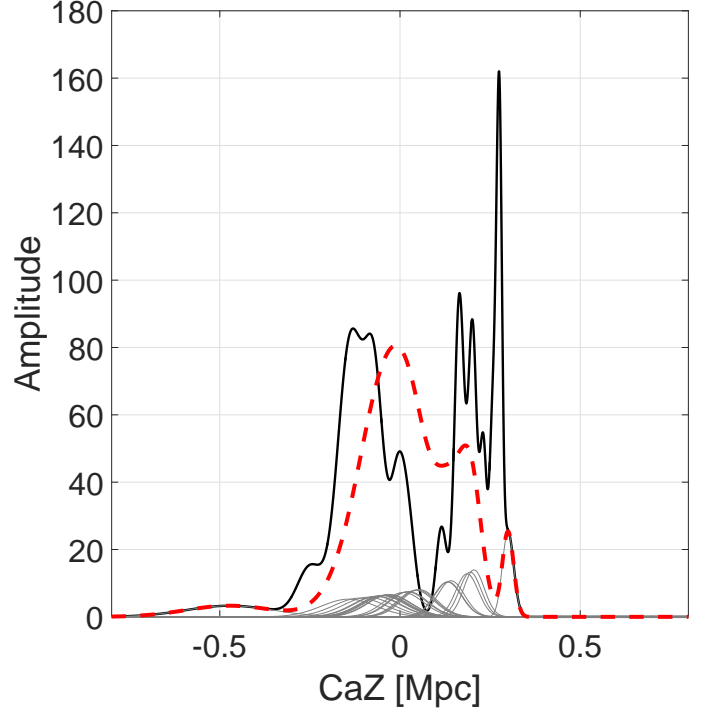


**Fig. 4.** Adaptive Kernel for the Cen A subgroup members. Shown is the density distribution of satellite galaxies along the CaZ axis from a superposition of projected standard normal curves taking care of distance uncertainties (see text). The black line corresponds to the *T15 sample* (members and candidates), the red dotted line to the *Candidate sample*, assuming a distance of 3.68 Mpc (Cen A) and an uncertainty due to the depth of the subgroup of  $\pm 0.5$  Mpc. The standard normal curves of the candidates are shown in grey.

It is now important to test the significance of the planar structures.

## 6. Statistical analysis

Is the seemingly bimodal structure of the Cen A subgroup statistically significant? To answer this question we performed two different statistical tests, the Anderson-Darling test (D'Agostino & Stephens 1986) and the Hartigan dip test (Hartigan & Hartigan 1985). The null hypothesis is that the observed galaxy distribution can be described by a unimodal normal distribution. Basically, we ask whether or not the galaxy distribution in the edge-on view, sampled along the CaZ axis, can be explained by a single normal distribution. If the null hypothesis is rejected, there must be evidence of multimodality in the Cen A subgroup, or the assumption of an underlying normal distribution is incorrect. We test the four samples listed in Table 1: (1) the *T15 sample*, (2) the *LV sample*, (3) the *Candidate sample*, and (4) the *Complete sample*.

The Anderson-Darling test is an improved version of the Kolmogorov-Smirnov test. Both compare the standard normal cumulative distribution function (CDF) with the empirical cumulative distribution function (ECDF) created from the data. If the difference between the ECDF and CDF becomes larger than a critical value, the hypothesis of nor-

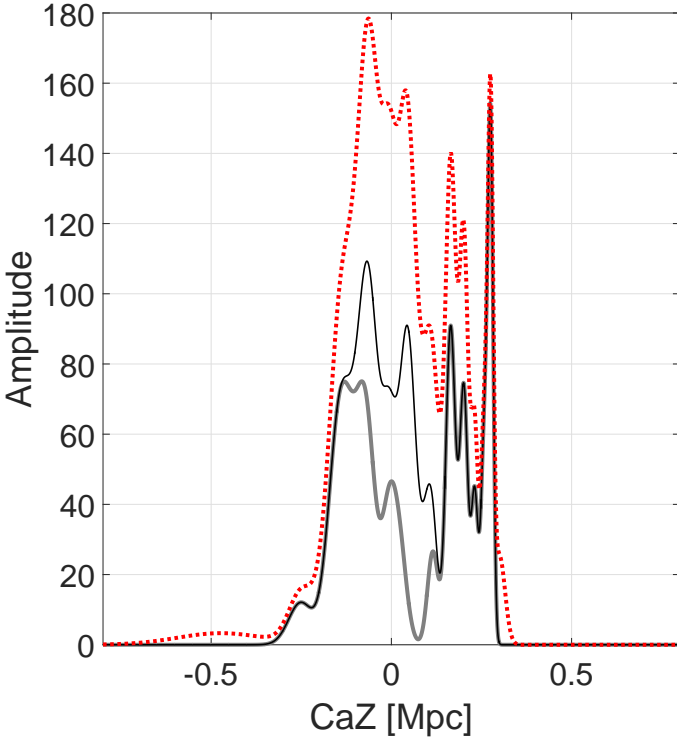


**Fig. 5.** Same as Fig. 4 but including the PISCeS dwarfs and shown as cumulative distribution, analogous to the histogram of Fig. 3. The grey line corresponds to the members of the two planes from the *T15 sample*. The black line corresponds to the *LV sample*, comprising the *T15 sample* plus the nine new dwarfs from the PISCeS survey, thus representing all known galaxies with distances  $< 1$  Mpc from Cen A. The red dotted line is the grand total, i.e. the superposition of the black line and all the possible members of the Cen A subgroup from the *Candidate sample* (Müller et al. 2016; Crnojević et al. 2016), assuming a distance of 3.68 Mpc (Cen A) and an error of  $\pm 0.5$  Mpc. The galaxy Cen A itself is located at CaZ=0.

mality is rejected with some significance level. In contrast to Kolmogorov-Smirnov, the Anderson-Darling test weights the tails of a distribution higher than the center. We use the implementation of the Anderson-Darling test provided by MATLAB.

The results for the Anderson-Darling test are presented in Table 4: samples (2), (3), and (4) pass the test for normality at the significance level of 5% with  $p_{AD}$ -values of 0.18, 0.07 resp. 0.15. With a  $p_{AD}$ -value of 0.07 the candidates-only sample (3) has still a marginal probability of not being unimodally distributed. Sample (1) is inconsistent with being drawn from a normal distribution with a  $p_{AD}$ -value of 0.02, an expected result given the finding of T15. Taking all the recently added data into account, however, the distribution of galaxies along the CaZ axis becomes consistent with being normally distributed.

There is a possible caveat. The footprint of the PISCeS survey does not cover the whole area on the sky taken by the two planes, see Fig. 2 of Müller et al. (2016), which could lead to a selection bias. Disregarding the findings of the PISCeS survey: Dw1, Dw2, Dw4, Dw8, and Dw9 would have been detected in the data of our Centaurus

group survey, but not the extremely faint and diffuse objects Dw5, Dw6, and Dw7. Furthermore, the photometric properties of the tidally disrupted dwarf Dw3 does not conform with our search criteria and would have remained undetected too. We also assume that Dw10, Dw11, Dw12, and Dw13 would not have been detected (no photometry was performed in Crnojević et al. (2016) for these candidates). In total, only five Dw galaxies would then feature in the *Candidate sample* and *Complete sample* with an assumed distance of 3.68 Mpc. Do the significance tests return different results with these conservative assumptions? We repeated the Anderson-Darling test with the following results: the null hypothesis is rejected for samples (1) and (2), while samples (3) and (4) are consistent with a normal distribution at the 5% confidence level. Sample (2) is rejected because it now contains only the galaxies with distances from the *T15 sample*. We therefore conclude that the outcome of the Anderson-Darling is little affected by a selection bias from including the PISCeS dwarfs in the analysis.

The Hartigan dip test provides another method to test for bimodality. It measures the maximum difference between the empirical distribution function and the unimodal distribution function that minimizes that maximum difference. We use an implementation originated by Hartigan (1985) which was translated into MATLAB by Ferenc Mechler.

The results for the Hartigan dip test are: samples (2), (3), and (4) pass the test at the significance level of 5% with  $p$ -values of 0.61, 0.72 resp. 0.84. Only sample (1) fails the test with a  $p$ -value of 0.00. This is the same result as before. Again we checked for a change of the results by the exclusion of the five candidates from the *T15 sample*. With a  $p$ -value of 0.08 the result for this plane-members-only subsample changes indeed. It now has a marginal probability of not being unimodally distributed. And when testing at a 10% significance level it is clearly rejected from unimodality. Overall the conclusion is hence the same: while the galaxy data used in the original analysis by Tully and collaborators support the picture of a multimodal distribution (two planes), adding the new galaxies, and thereby doubling the sample, presents a picture that is consistent with a unimodal normal distribution.

Until now no distance uncertainties were taken into account when testing for the significance of the planes. To test whether these results are indeed representative of the data and their uncertainties, we performed Monte Carlo simulations where the distance of a galaxy is randomly taken from a normal distribution with  $\mu$  given by the galaxy position and  $\sigma$  by the distance error of 5 %. Remember that we sample along the CaZ axis, which means that we only count the CaZ component of the distance uncertainty. For galaxies without distance measurements a conservative distance uncertainty of  $\pm 0.5$  Mpc, accounting for the depth of the Cen A subgroup, is taken. We calculated 10000 realizations of all samples and applied both the Anderson-Darling and the Hartigan dip test on them. The resulting probabilities that the null hypothesis (= normal distributed) is rejected for the Anderson Darling and the Hartigan dip test, respectively, are as follows: (1) is rejected in 66 and 62 percent of the draws, (2) in 2 and 0 percent, (3) in 21 and 0 percent, and (4) in 5 and 0 percent.

In this analysis all candidates are considered to be satellites of Cen A. But what if some of them are not members

of the Cen A subgroup but lie in the background? To check this possibility, we broadened the distance uncertainty to  $\pm 1.5$  Mpc and repeated the MC runs. Remember that we exclude all galaxies with radial distance to Cen A larger than 1 Mpc. When we rerun the simulations with this setup, (1) gets rejected in 65 and 56 percent of the cases, (3) in 18 and 2 percent, and (4) in 5 and 0 percent. Hence this wider spread essentially lowers the rejection rate.

The results of these tests are summarized in Table 4. Column 1: Test sample name. Columns 2+3: accepted hypothesis and  $p$ -value from the Anderson-Darling test. Column 4: Probability for a rejection of  $h_0$  estimated with the Anderson-Darling test from Monte Carlos simulations. In brackets are the results from the test with a distance uncertainty of  $\pm 1.5$  Mpc. Columns 5+6: accepted hypothesis and  $p$ -value from the Hartigan dip test. Column 7: Probability for a rejection of  $h_0$  estimated with the Hartigan dip test from Monte Carlos simulations. In brackets are the results from the test when adopting a distance uncertainty of 1.5 Mpc.

**Table 4.** Anderson-Darling and Hartigan dip test results.

Sample	$h_{AD}$	$p_{AD}$	$P_{AD, MC}$	$h_{dip}$	$p$	$P_{dip, MC}$
(1)	$h_1$	0.02	0.66 (0.65)	$h_1$	0.00	0.62 (0.56)
(2)	$h_0$	0.18	0.02	$h_0$	0.61	0.00
(3)	$h_0$	0.07	0.21 (0.18)	$h_0$	0.72	0.01 (0.02)
(4)	$h_0$	0.15	0.05 (0.06)	$h_0$	0.84	0.00 (0.00)

**Notes.**  $h_0$  means that the null hypotheses of normal distribution passes the test,  $h_1$  means it is rejected. It is rejected when  $p \leq 0.05$ .

From all our results we conclude that with the addition of the new data the significance against a unimodal distribution of the satellites around Cen A rises, i.e. the significance for bimodality is weakened, even though the case for a double-plane structure as suggested T15 is not completely ruled out.

We performed one last test. What would happen, if the new candidates were exactly lying in (one of) the two planes? To find out, we calculated the intersection point between the line of sight and the planes, and thus a new (hypothetical) distance  $d_{inter}$  for each candidate from the *Candidate sample* and the *Complete sample*. To account for the thickness of the planes, we also calculated the intersection points at  $\pm$  the r.m.s. thickness of the planes, giving a minimal ( $d_{min}$ ) and maximal ( $d_{max}$ ) value for the distance. Remember that we only take galaxies into account where the radial distance between the galaxy and Cen A is less than 1 Mpc. In Table 5 we present the estimated distances for all galaxies, where at least one of the three intersection points is closer than 1 Mpc to Cen A. Distances marked with an asterisk are outside of this 1 Mpc radius. The following eight candidates miss the two planes in the 1 Mpc vicinity of Cen A and are therefore removed from the modified *Candidate* and *Complete samples*: dw1329-45, CenA-MM-Dw13, dw1331-40, dw1337-41, KK198, KKs54, KKs59, and KKs51.

**Table 5.** Predicted distances for the candidates.

Name	$d_{inter}$ [Mpc]	$d_{min}$ [Mpc]	$d_{max}$ [Mpc]
Plane 1			
dw1315-45	3.84	3.53	4.15
dw1318-44	4.07	3.75	4.40
CenA-MM-Dw11	4.15	3.82	4.45
dw1322-39	3.83	3.52	4.13
dw1323-40c	4.07	3.75	4.40
dw1323-40b	4.13	3.80	4.46
CenA-MM-Dw12	4.37	4.02	4.72*
dw1323-40	4.26	3.92	4.60
dw1326-37	4.01	3.70	4.33
CenA-MM-Dw10	4.99*	4.59	5.39*
dw1330-38	4.86*	4.47	5.25*
dw1331-37	4.85*	4.46	5.23*
Plane 2			
dw1336-44	2.26*	1.78*	2.74
dw1337-44	2.36*	1.86*	2.87
dw1341-43	3.29	2.59*	4.00
dw1342-43	3.51	2.76	4.26
KKs58	3.02	2.38*	3.67

Applying the Anderson-Darling and Hartigan dip tests to the modified *Candidate sample* and *Complete sample* leads to the following changes: (3) and (4) are now rejected by the Anderson-Darling test both with a  $p_{AD}$ -value of 0.00. The same is true when testing with  $d_{min}$  and  $d_{max}$ . On the other hand, the Hartigan dip test still accepts the null hypotheses for samples (3) and (4), as before, but the  $p$ -values are lowered to 0.08 and 0.66, respectively. Again, we get the same result when testing with  $d_{min}$  and  $d_{max}$  instead of  $d_{inter}$ . With a  $p$ -value of 0.08, the modified *Candidate sample* is now marginally significant of not being unimodal, whereas the modified *Complete sample* gives a strong hint for unimodality, in contrast to the Anderson-Darling test.

Hypothetically, putting the new candidates onto the best-fitting planes must of course strengthen the case for the planes. But as we cannot exclude the possibility that the dwarfs are indeed lying in the planes without accurate distance measurements, we also cannot conclusively rule out the reality of the planes.

## 7. Discussion and Conclusion

The discovery of a large number of new dwarf galaxies in the nearby Centaurus group (Crnojević et al. 2014, 2016; Müller et al. 2015, 2016) openend the opportunity to conduct a significance test of the two planes of satellites reported by Tully et al. (2015). While this normally requires follow-up observations to measure galaxy distances, in the case of the Cen A subgroup, due to the special geometric situation, one can take advantage of the fact that the line of sight from our vantage point runs along the postulated planes of satellites. Therefore, galaxies even without distance measurements can be used for the test, as distance uncertainties will move galaxies along or parallel to the planes. In other words, distance uncertainties produce only little crosstalk between the planes and the space around them. This allows to include all Cen A member candidates in the analysis, which doubles the sample size from 30 to 59.

Sampling galaxy positions along an edge-on projection of the planes we studied the distribution of Cen A subgroup members by two different techniques, a histogram and a more sophisticated adaptive kernel density estimation. A gap, or dip in the distribution marking the two planes is visible in both representations of the data. However, it is also quite evident that with the inclusion of the new galaxy data the gap between the two planes starts to be filled, raising the conjecture that the “two plane” scenario around Cen A might be an artifact of low number statistics. To put this under statistical scrutiny, we performed an Anderson-Darling test and a Hartigan dip test to see whether the distribution is in agreement with a unimodal normal distribution. We find that both tests fail with the sample used by Tully et al. (2015), rejecting the unimodal normal hypothesis for that original sample. This result is consistent with their finding that the satellites can be split into two planes. However, with the addition of the new dwarf members and candidates of the Cen A subgroup, the deviation from a normal distribution loses statistical significance in the sense of the two tests applied. Hence it is now conceivable that the satellites follow a normal distribution, and the gap between the two planes is indeed an artefact from small number statistics. We performed Monte Carlos simulations to further strengthen these results by taking distance uncertainties into account and find that the results change only marginally.

Given that distance measurements for the candidate galaxies are unavailable at the moment, it is theoretically possible to allocate 17 out of 25 galaxies to one of the two planes each by moving them along the line of sight. That means, technically the existence of the two planes cannot be completely ruled out at this point. Only distance measurements will tell whether the candidates lie on or near the planes. All we can say is that the case for two planes around Cen A is weakened by including the currently available data for 29 new dwarfs and dwarf candidates.

Another, at first glance secondary result of our testing is that, in parallel with the weakening of the significance for bimodality, the galaxy population in plane 1 has now become dominant. This is not surprising: Cen A lies closer to plane 1 in projection ( $\text{CaZ}=0$  in Fig. 5), such that any newly discovered satellite galaxy in a distribution radially concentrated on Cen A will necessarily result in an additional member of plane 1 than plane 2. However, this amassing of Cen A satellites in the proposed plane 1 is important, as the planarity of “Plane 1” has not been destroyed by adding the candidates. The alignment of the tidally disrupted CenA-MM-Dw3 with plane 1 (see Figs. 1 and 2) is intriguing too. The Cen A plane 1 is certainly a good *candidate analog* of the local thin planes detected around the Milky Way (VPOS) and the Andromeda galaxy (GPOA). Future distance measurements for the many new Cen A subgroup member candidates will be able to tell how far the analogy will take us.

**Acknowledgements.** OM, HJ, and BB are grateful to the Swiss National Science Foundation for financial support. HJ acknowledges the support of the Australian Research Council through Discovery projects DP120100475 and DP150100862. MSPs contribution to this publication was made possible through the support of a grant from the John Templeton Foundation. The opinions expressed in this publication are those of the authors and do not necessarily reflect the views of the John Templeton Foundation.

## References

Cautun, M., Bose, S., Frenk, C. S., et al. 2015, MNRAS, 452, 3838  
 Chiboucas, K., Jacobs, B. A., Tully, R. B., & Karachentsev, I. D. 2013, AJ, 146, 126  
 Chiboucas, K., Karachentsev, I. D., & Tully, R. B. 2009, AJ, 137, 3009  
 Crnojević, D., Sand, D. J., Caldwell, N., et al. 2014, ApJ, 795, L35  
 Crnojević, D., Sand, D. J., Spekkens, K., et al. 2016, ApJ, 823, 19  
 D’Agostino, R. B. & Stephens, M. A. 1986, Goodness-of-fit techniques  
 Golub, G. & Kahan, W. 1965, SIAM Journal on Numerical Analysis, 2, 205  
 Hartigan, J. A. & Hartigan, P. M. 1985, The Annals of Statistics, 13, 70  
 Hartigan, P. M. 1985, Journal of the Royal Statistical Society. Series C (Applied Statistics), 34, 320  
 Hui, X., Ford, H. C., Freeman, K. C., & Dopita, M. A. 1995, ApJ, 449, 592  
 Ibata, N. G., Ibata, R. A., Famaey, B., & Lewis, G. F. 2014a, Nature, 511, 563  
 Ibata, R. A., Ibata, N. G., Lewis, G. F., et al. 2014b, ApJ, 784, L6  
 Ibata, R. A., Lewis, G. F., Conn, A. R., et al. 2013, NAT, 493, 62  
 Javanmardi, B., Martinez-Delgado, D., Kroupa, P., et al. 2016, A&A, 588, A89  
 Karachentsev, I. D., Karachentseva, V. E., Huchtmeier, W. K., & Makarov, D. I. 2004, AJ, 127, 2031  
 Karachentsev, I. D., Makarov, D. I., & Kaisina, E. I. 2013, AJ, 145, 101  
 Koch, A. & Grebel, E. K. 2006, AJ, 131, 1405  
 Libeskind, N. I., Hoffman, Y., Tully, R. B., et al. 2015, MNRAS, 452, 1052  
 Merritt, A., van Dokkum, P., & Abraham, R. 2014, ApJ, 787, L37  
 Metz, M., Kroupa, P., & Jerjen, H. 2007, MNRAS, 374, 1125  
 Müller, O., Jerjen, H., & Binggeli, B. 2015, A&A, 583, A79  
 Müller, O., Jerjen, H., & Binggeli, B. 2016, ArXiv e-prints  
 Pawłowski, M. S. 2016, MNRAS, 456, 448  
 Pawłowski, M. S., Famaey, B., Jerjen, H., et al. 2014, MNRAS, 442, 2362  
 Pawłowski, M. S., Famaey, B., Merritt, D., & Kroupa, P. 2015a, ApJ, 815, 19  
 Pawłowski, M. S., Kroupa, P., & Jerjen, H. 2013, MNRAS, 435, 1928  
 Pawłowski, M. S., McGaugh, S. S., & Jerjen, H. 2015b, MNRAS, 453, 1047  
 Pawłowski, M. S., Pfleiderer-Altenburg, J., & Kroupa, P. 2012, MNRAS, 423, 1109  
 Phillips, J. I., Cooper, M. C., Bullock, J. S., & Boylan-Kolchin, M. 2015, MNRAS, 453, 3839  
 Sand, D. J., Crnojević, D., Strader, J., et al. 2014, ApJ, 793, L7  
 Tully, R. B. 2015, AJ, 149, 171  
 Tully, R. B., Libeskind, N. I., Karachentsev, I. D., et al. 2015, ApJ, 802, L25